Free Radical Biology and Medicine 190 (2022) 226–233

Contents lists available at ScienceDirect

Free Radical Biology and Medicine

journal homepage: www.elsevier.com/locate/freeradbiomed

Noninvasive detection of the endogenous free radical melanin in human skin melanomas using electron paramagnetic resonance (EPR)

Lionel Mignion [a,b], Celine M. Desmet [a], Evelyne Harkemanne [c], Isabelle Tromme [c], Nicolas Joudiou [a,b], Mohammad Wehbi [a], Jean-François Baurain [d], Bernard Gallez [a,*]

[a] Louvain Drug Research Institute, Biomedical Magnetic Resonance Research Group, Université Catholique de Louvain (UCLouvain), Brussels, Belgium
[b] Louvain Drug Research Institute, Nuclear and Electron Spin Technologies Platform, Université Catholique de Louvain (UCLouvain), Brussels, Belgium
[c] Dermatology Department, Cliniques Universitaires Saint-Luc, Brussels, Belgium
[d] Medical Oncology Department, Cliniques Universitaires Saint-Luc, Brussels, Belgium

ARTICLE INFO

Keywords:
Electron Paramagnetic Resonance (EPR)
Melanoma
Nevi
Diagnostic
Melanin

ABSTRACT

We explored the capability of low-frequency Electron Paramagnetic Resonance (EPR) to noninvasively detect melanin (a stable semiquinone free radical) in the human skin. As previous *in vitro* studies on biopsies suggested that the EPR signal from melanin was different when measured in skin melanomas or benign nevi, we conducted a prospective first-in-man clinical EPR study in patients with skin lesions suspicious of melanoma. EPR spectra were obtained using a spectrometer operating at 1 GHz, with a surface coil placed over the area of interest. Two clinical studies were carried out: 1) healthy volunteers ($n = 45$) presenting different skin phototypes; 2) patients ($n = 88$) with skin lesions suspicious of melanoma ($n = 100$) requiring surgical resection. EPR data obtained before surgery were compared with histopathology results. The method was not sensitive enough to measure differences in melanin content due to changes in skin pigmentation. In patients, 92% of the spectra were analyzable. The EPR signal of melanin was significantly higher ($p < 0.0001$) in melanoma lesions ($n = 26$) than that in benign atypical nevi ($n = 62$). A trend toward a higher signal intensity (though not significant) was observed in high Breslow depth melanomas (a marker of skin invasion) than in low Breslow lesions. To date, no naturally occurring free radicals have been detected by low-frequency EPR systems adapted for clinical studies. Here, we demonstrated for the first time the ability of this technology to detect an endogenous free radical, opening new avenues for evaluating clinical EPR as a potential aid in the diagnosis of pigmented skin lesions.

1. Introduction

Electron Paramagnetic Resonance (EPR) or, equivalently, Electron Spin Resonance (ESR) is a magnetic resonance technology that characterizes paramagnetic species that contain unpaired electrons. Most standard EPR spectrometers operate at higher frequencies (9 GHz, microwave range) and lower fields (sweep around 0.3 T) than conventional NMR spectrometers (radiofrequency range). At this high frequency, the nonresonant absorption of electromagnetic radiation by aqueous samples presents a serious problem, thus limiting the sample size to a thickness of less than 1 mm. Non-invasive analysis of tissues from animals or humans can be achieved only by reducing the operating frequency (1 GHz or lower), which dramatically affects the signal-to-noise ratio and the capability of EPR to detect paramagnetic compounds *in vivo*. The construction of whole-body clinical EPR systems and adapted resonators [1,2] has recently opened the possibility of applying EPR to healthy volunteers and patients [3,4]. To date, *in vivo* applications of clinical EPR have been restricted to oximetry [5,6] and retrospective dosimetry [7,8]. In EPR oximetry, a paramagnetic sensor is administered to the tissue of interest, and the oxygen-dependent variation of the spectrum is analyzed to provide measurements of tissue oxygenation [9]. In EPR dosimetry, stable carbonate free radicals generated within the hydroxyapatite matrix of the enamel are detected to assess the radiation dose [10]. Thus far, it has been considered that naturally occurring compounds with unpaired electrons are present in insufficient amounts for detection by low-frequency clinical EPR systems. The main objective of the present study was to meet the challenge of detecting noninvasively the endogenous free radical melanin as a potential

* Corresponding author. Biomedical Magnetic Resonance Research Group, Louvain Drug Research Institute, Université catholique de Louvain (UCLouvain), Avenue Mounier 73.08, B-1200, Brussels, Belgium.
E-mail address: bernard.gallez@uclouvain.be (B. Gallez).

https://doi.org/10.1016/j.freeradbiomed.2022.08.020
Received 25 June 2022; Received in revised form 5 August 2022; Accepted 12 August 2022
Available online 18 August 2022

diagnostic aid of pigmented skin lesions.

Melanin is produced by melanocytes that are spread throughout the lower part of the epidermis or in clusters (nevi). Melanin is a mixture of polymers containing indoles and other intermediate products derived from the oxidation of tyrosine [11–13]. Eumelanin is a brown-black pigment, whereas pheomelanin is a yellow reddish-brown pigment. Both pigments are stable semi-quinone free radicals with distinct EPR spectra [14]. It has been generally accepted that eumelanin is the main pigment present in melanomas due to the overexpression of the tyrosinase gene, a key gene in eumelanogenesis [11,15]. However, other studies have shown that pheomelanin might also be present in variable concentrations in human melanoma samples [16–18]. EPR spectrometry and imaging using high-frequency spectrometers (9 GHz) have been successfully applied for the detection of melanin *in vitro* in paraffin-embedded melanoma slices and frozen melanoma samples [18–26]. Using low-frequency EPR (1 GHz), we have previously succeeded in noninvasively detecting the signal from melanin in mice bearing B16 melanomas [26,27], including using a clinical EPR device [27], paving the way for the present study.

The motivation for performing a prospective clinical trial using clinical EPR on pigmented skin lesions suspected of melanoma was based on a study carried out by Cesareo on human biopsies [28]. These authors performed EPR analysis *in vitro* (9 GHz) on paraffin-embedded human melanoma and nevi sections. They observed that the EPR signal in nevi was significantly lower than that in melanomas and found a correlation between the EPR signal and Breslow depth (tumor thickness in the skin) [28]. Breslow depth is a strong indicator of increased metastatic potential of the tumor, and patient management depends on its value. Thus, in clinical practice, lesions suspicious for melanoma are first excised with minimal margins to confirm the diagnosis and histopathologically measure the Breslow depth. When the Breslow thickness is larger than 0.8 mm (high Breslow), a sentinel lymph node biopsy is recommended in addition to a second surgery to enlarge the margins of resection [29,30]. Non-invasive information on the Breslow depth before excision would inform the dermatologist on the emergency of surgery, provide guidance on resection margins, and accelerate patient management regarding the need for lymph node analysis.

The ultimate goals of the present study were to assess the feasibility of noninvasive detection of melanin by low-frequency EPR in suspicious pigmented skin lesions, evaluate the value of the technology to discriminate between benign and malignant lesions, and compare the EPR signal recorded with the Breslow depth measured by histopathology. We first validated a procedure to analyze the EPR melanin signal with a very weak signal-to-noise ratio from phantoms placed at the surface of water samples and human skin. We then applied the procedure to healthy volunteers (n = 45) to assess the influence of the phototype (classification of the skin by its pigmentation and reaction to sunlight exposure) on the EPR signal. Finally, we conducted a prospective first-in-man clinical EPR study in patients with suspicious pigmented skin lesions (n = 100) requiring surgical resection to compare EPR data with histopathological results.

2. Materials and methods

2.1. EPR acquisition parameters

EPR measurements were performed on a whole-body clinical EPR system (Clin-EPR LLC, Lyme, NH) operating at 1.15 GHz (pole gap of the magnet = 50 cm). The area of interest (phantom at the surface of a water sample or skin, normal skin, or skin lesion) was placed at the center of the magnet below a loop-gap surface coil resonator with an inner diameter of 8 mm [31]. A film (Parafilm®"M," Neenah, WI, USA) 10 × 20 cm was folded eight times and placed between the coil and the sample of interest. The coil touched the area of interest under a light pressure. Measurements were performed with the following parameters: center field, 41.6 mT; modulation amplitude, 0.3 mT; microwave power, 10 mW; time constant, 5 ms; scan time, 5 s; scan range, 4 mT. Tuning was checked after acquisition of two spectra. A sealed capillary containing 10 μL of a 2 mM solution of ^{15}N-PDT (4-oxo-2,2,6,6-tetramethylpiperidine-d_{16}-^{15}N-1-oxyl; CDN Isotopes, Pointe-Claire, Canada) was fixed along the axis of the resonator with the tip of the capillary just at the surface of the loop coil. Before each measurement, the coil was protected using a single-use disposable Rinn® Universal Digital Sensor Cover (Elgin, IL, USA).

2.2. Melanin phantoms and calibrations

Solid dilutions of melanin (> Sepia officinalis, >99%; Sigma-Aldrich, Steinheim, Germany) were performed by trituration with increasing amounts of sucrose (>99%, Fluka Biochemika, Steinheim, Germany). The powder was weighed on Scotch® Magic tape with melanin content varying between 0.075 mg and 1 mg. The diameter of the circle occupied by the powder was selected as less than 8 mm (diameter of the loop coil). After weighing, the tape was covered with another tape and the obtained film was used for calibration purposes. For *in vitro* calibrations, films containing melanin were placed on the surface of a NaCl 0.9% water bag (Baxter, Lessines, Belgium), and 10 independent EPR measurements were performed by acquisition of five series of two scans of the whole EPR spectrum (to visualize the signals from ^{15}N-PDT and melanin). For *in vivo* measurements, films containing melanin were taped onto the surface of the forehead skin, and five independent EPR measurements were performed. Each measurement included nine series of 2 spectra. In addition, the reproducibility of the EPR measurements was tested by placing a phantom containing melanin on the surface of the skin in six different body positions of the same healthy volunteer (right forearm, left forearm, right leg, left leg, forehead, and shoulder). Ten independent EPR measurements were performed for each body position.

2.3. Clinical trial: EPR on skin belonging to different phototypes

The EPR signal of melanin was characterized in healthy skin presenting different phototypes to assess the potential influence of skin pigmentation on the EPR signal. The clinical trial (Eudra-CT 2018-004203-39) was approved by the *Comité d'éthique hospitalo-facultaire (CEHF) des Cliniques universitaires Saint-Luc (CUSL)* on January 11, 2019, and by the Belgian Federal Agency for Medicines and Health Products on January 18, 2019. Forty-five healthy volunteers with a minimum age of 18 years were recruited between March 22, 2019, and September 17, 2019. They were recruited by the Biomedical Magnetic Resonance Laboratory from among students and faculty members of the Health Sector of UCLouvain by responding to a recruitment advertisement. The candidates had to fill a questionnaire based on skin pigmentation and reaction to sunlight exposure to classify their skin phototypes according to the Fitzpatrick scale [32] (phototype I: pale white skin, freckled, blue/green eyes, blond/red hair, always burns, does not tan; Phototype II: fair skin, blue eyes, burns easily, tans poorly; Phototype III: white to light brown skin, tans after initial burn; Phototype IV: light to moderate brown skin, burns minimally, tans easily; Phototype V: brown skin, rarely burns, tans darkly easily; Phototype VI: dark brown or black skin, never burns, always tans darkly). They filled the informed consent before enrollment. The recruitment included 15 persons with phototype I-II, 15 persons with phototype III-IV, and 15 persons with phototype V-VI. The exclusion criteria were as follows: individuals with pacemakers or metal implants, claustrophobic or agitated individuals, and pregnant women (a β-HCG urinary test was performed to ensure the absence of pregnancy in non-menopausal women). The subjects were placed over a wheeling aluminum bed covered with a stretcher mattress protected by disposable single-use paper. The forearm of the healthy volunteer was positioned behind the head, and the coil was placed over the area of interest with light pressure at the center of the magnet. The area analyzed was exempt from any lesions, and the skin was protected with Parafilm, as described

previously. A series of EPR scans were recorded using the acquisition parameters described previously. During the acquisitions, we checked the presence of the two reference peaks coming from ^{15}N-PDT. In practice, we sought to acquire at least 15 EPR scans with reasonable signal-to-noise ratio from ^{15}N-PDT. No adverse events or serious adverse events were reported in the clinical trial.

2.4. Clinical trial: EPR on suspicious skin lesions

The clinical trial (Eudra-CT 2017-002503-94) was approved by the *Comité d'éthique hospitalo-facultaire des Cliniques universitaires Saint-Luc* on June 21, 2018, and by the Belgian Federal Agency for Medicines and Health Products on August 9, 2018. Eighty-eight patients (presenting a total of 100 lesions) were recruited between November 22, 2019, and April 25, 2022, with an interruption in recruitment from March 2020 to September 2021 due to the SARS-Cov-2 pandemic. The objective of the clinical trial was to assess the feasibility of detecting the EPR signal of melanin in melanocytic lesions and to correlate the EPR signal with standard histological analysis of excised lesions by the anatomopathology department of the CUSL. Inclusion criteria were patients with lesions suspicious for melanoma requiring surgical resection with the lesion in an area that could be positioned in the center of the EPR magnet and allowing the positioning of an antenna touching its surface. A minimum age of 18 years was required. The patients were recruited by dermatologists from the Dermatology Department of the *CUSL*. Before enrollment, the candidates provided informed consent. The exclusion criteria were the same as those described previously. The lesion was covered with parafilm and placed at the center of the magnet, as described previously. The surface coil was placed over the lesion under light pressure. EPR spectra were recorded with the acquisition parameters described previously using a series of two spectra with a 5 s acquisition time. After tuning the coil, the patients were required to remain immobile. When the lesion was present in the abdominal, chest, or back areas, patients were required to hold their breath for 10 s up to the end of the acquisition. A series of EPR scans were recorded using the acquisition parameters described previously. During the acquisitions, we checked the presence of the two reference peaks coming from ^{15}N-PDT. In practice, we sought to acquire at least 15 EPR scans with reasonable signal-to-noise ratio from ^{15}N-PDT. No adverse events or serious adverse events were reported in the clinical trial.

2.5. EPR data analysis

The data were processed using the homebuilt MATLAB code provided in the supplementary materials. The first step included a quality check of all individual EPR spectra recorded and the removal of spectra where an obvious motion was noted (instability or sudden change in the baseline) and/or an absence of the PDT reference signals. The median EPR spectrum was calculated. The baseline of the median EPR spectrum was then corrected and the first integration was calculated using cumulative trapezoidal numerical integration (cumptrapz function). Finally, a polynomial function was used before calculating the second integration (see the MATLAB code in the supplementary materials). The results were expressed as the ratio between the double integrated signal of the melanin peak divided by the double integrated signal of the two PDT peaks.

3. Results

3.1. Setup and validation of the procedure to measure eumelanin at the surface of the skin

EPR spectra were recorded on a whole-body EPR spectrometer operating at 1.15 GHz. Phantoms of melanin or skin areas of interest (protected by a plastic film) were placed under a surface-loop resonator, as shown in Fig. 1. Eumelanin displayed a single EPR line characterized by a g-factor of approximately 2.004. A previous analysis of eumelanin content in primary skin melanomas (based on the formation of pyrroletricarboxylic acid through permanganate oxidation) suggested concentrations in the range 0.3–4.5 mg/g of tissue [17]. As the volume of interest under the coil (diameter of 8 mm) was lower than 1 cm^3, we prepared flat phantoms with eumelanin content varying between 0.075 mg and 1.0 mg. The analysis of phantoms with decreasing amounts of eumelanin revealed that the 1st-derivative EPR signal becomes difficult to analyze in terms of position and intensity using rapid acquisition for the analysis of lesions in patients (Fig. 2). Indeed, as the analyzed suspicious skin lesions could be located in areas prone to motion (abdomen, chest), we limited the acquisition time to a series of two spectra recorded in 5 s, compatible with a breath hold of 10 s. To allow the unambiguous analysis of eumelanin, we used a stable nitroxide (^{15}N-PDT or 4-oxo-2,2,6,6-tetramethylpiperidine-d$_{16}$-^{15}N-1-oxyl) in a sealed capillary fixed to the resonator. The EPR signal from this nitroxide is a doublet due to the coupling of the electron spin with ^{15}N, which possesses a nuclear spin I = ½. This signal was used as a reference for field positioning, as the melanin signal appeared between both lines (Fig. 2), and for quantitative purposes (ratio between variable amounts of melanin and fixed amount of ^{15}N-PDT). We developed a MATLAB program for the analysis of samples with very low eumelanin contents. The analysis included the following steps: quality check of all individual EPR spectra and removal of spectra with obvious motion and/or absence of a reference signal, median spectrum, baseline correction, first integration using cumulative trapezoidal numerical integration, and polynomial fitting of the baseline and double integration. This process is illustrated in Fig. 3, using the analysis performed on a melanoma lesion (patient #85). The eumelanin

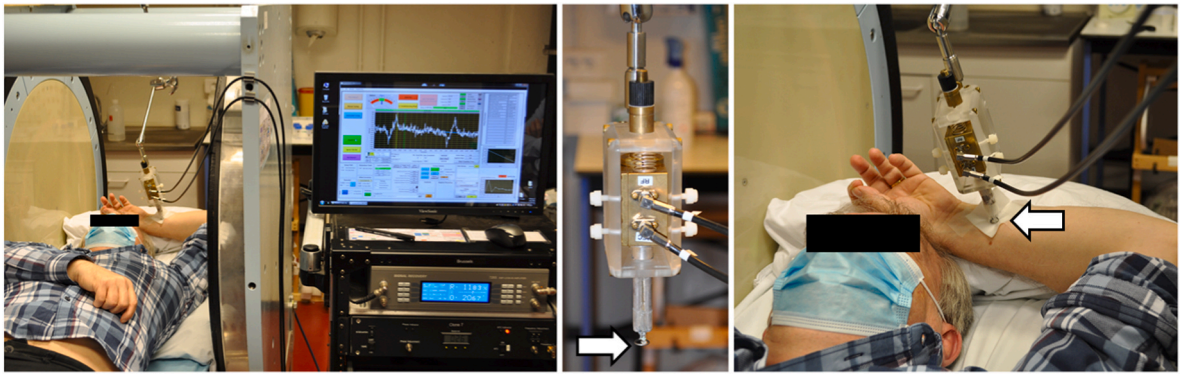

Fig. 1. Experimental set-up used for the present investigation. Left: Clinical EPR system with the subject lying between the poles of a magnet (field sweeping around 41 mT) and the computer interface allowing the visualization of the EPR spectra. Center: Resonator with the surface loop coil. Right: The coil is positioned over the area of interest covered by a plastic film and placed in the center of the magnet. The arrows show the surface loop coil.

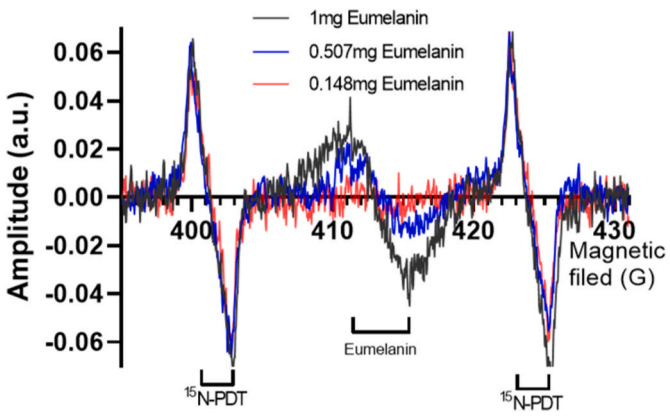

Fig. 2. EPR spectrum of melanin and PDT used as reference in a L-Band EPR clinical system. Typical spectra of eumelanin present in small amounts in phantoms placed under a surface coil in the L-Band clinical EPR system. At low concentration, the EPR signal becomes difficult to detect. For the analysis, ^{15}N-PDT in a sealed capillary was used as a reference. The EPR signal from PDT is a doublet with peaks located at lower and higher fields than the melanin signal. This signal was used as a reference for field positioning as the melanin signal appears between both lines and for quantitative purpose.

content was quantitatively assessed using a calibration built with phantoms placed on the surface of a water bag and on the forehead of a volunteer. A linear relationship was observed between the relative EPR signal intensity (melanin/PDT ratio) and the melanin content in the samples (Fig. 4A). The squares of the correlation coefficients were 0.9392 ($p < 0.0001$, Pearson correlation) and 0.9442 ($p < 0.0001$, Pearson correlation) for calibrations established at the surface of the waterbag and human skin, respectively. No significant differences were observed between calibration curves (Fig. 4A). In addition, a reproducibility assay was performed using the same phantom measured during ten different sessions and in six different body positions (left arm, right arm, left leg, right leg, shoulder, and forehead). No significant differences were observed in the relative signal intensity between the different positions ($p = 0.22$, one-way ANOVA) (Fig. 4B). The overall coefficient of variation for these measurements on the skin was 25%.

3.2. Influence of the skin phototype on the EPR signal

The first clinical study was conducted to analyze the influence of skin pigmentation on EPR signals recorded using the clinical EPR system. Forty-five healthy volunteers were recruited, belonging to phototypes I/II ($n = 15$), III/IV ($n = 15$), and V/VI ($n = 15$) according to the Fitzpatrick scale [31]. Measurements were performed on one arm of individuals in a region showing no skin lesions. No significant difference in EPR signal intensity was observed between the different phototype groups ($p = 0.75$, one-way ANOVA, Fig. 5). These results indicate that the present configuration of the L-band spectrometer used in this study was not sufficiently sensitive to measure the differences in melanin content due to changes in skin pigmentation. This indicated that pigmentation does not play a role in the evaluation of melanin content in skin lesions.

3.3. Link between the lesion status, the Breslow depth of the lesion and the EPR signal

The second study was a prospective clinical trial that included patients with skin lesions suspicious of melanoma requiring surgical resection. The patients underwent EPR examination immediately before surgery. The results of EPR analysis were compared with the diagnosis made in the histopathology report. A table summarizing the patients' characteristics is provided in the supplementary material, including sex, age, phototype, size and position of the lesion, histopathological diagnosis, and Breslow depth (if relevant). Images of all individual lesions and their respective EPR spectra are also presented. The study cohort included 88 patients (mean [SD] age, 55.1 [14.9] years; 44 women [50%]/44 men [50%], with a total of 100 suspicious lesions. Of these

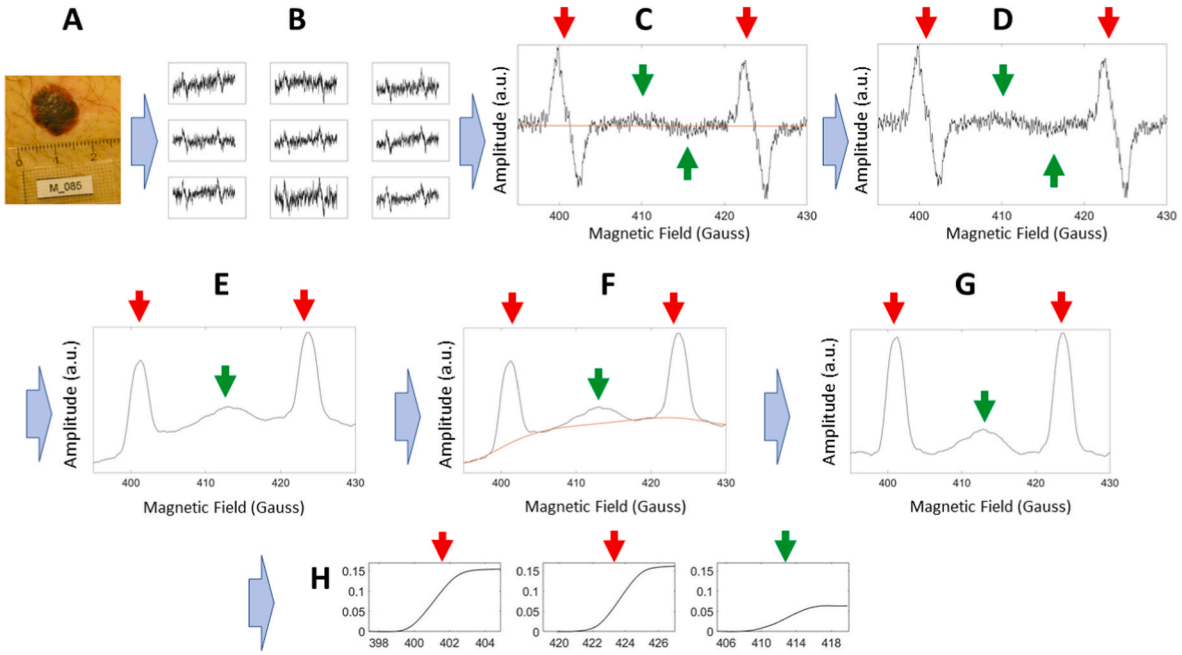

Fig. 3. Steps in EPR analysis of the melanin content in lesions. The example illustrated is from a melanoma in Patient #85. A: lesion of interest that was positioned in the center of the magnet under the surface loop resonator. B: visualization of a series of individual EPR spectra. This step allows to remove spectra with obvious motion of absence of reference peaks. C: median EPR spectrum obtained from spectra kept for the analysis. At this stage, a baseline correction is applied. The signal of melanin is shown with green arrows and PDT peaks with red arrows. D: median spectrum after baseline correction. E: raw first integrated EPR spectrum. F: polynomial fitting. G: corrected first integrated spectrum. H: second integrated spectra of the peaks of PDT (red arrows) and melanin (green arrow). (For interpretation of the references to colour in this figure legend, the reader is referred to the Web version of this article.)

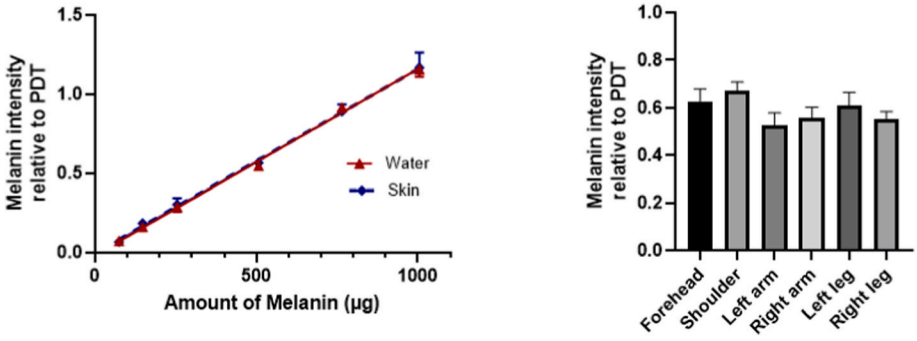

Fig. 4. Validation of the method to quantify melanin. Left: *in vitro* calibrations established with films containing melanin placed at the surface of a NaCl 0.9% water bag or the skin forehead of a healthy volunteer. Each point is the mean of 5 different measurements ± standard error. The squares of the correlation coefficients were 0.9392 ($p < 0.0001$, Pearson correlation) and 0.9442 ($p < 0.0001$, Pearson correlation) for calibrations established at the surface of water bag and human skin, respectively. No significant difference was observed between both calibration curves. Right: reproducibility assay using a film containing 0.507 mg melanin at the surface of the skin in 6 different body positions of a healthy volunteer (right forearm, left forearm, right leg, left leg, forehead, shoulder). Ten independent EPR measurements were done in each body position. Each independent measurement in the reproducibility assay included 9 series of 2 EPR spectra. Results are expressed as mean of the melanin signal intensity relative to PDT ± standard error. No significant difference was observed in the EPR signal intensity whatever the position of the measurement ($p = 0.22$, One-way Anova).

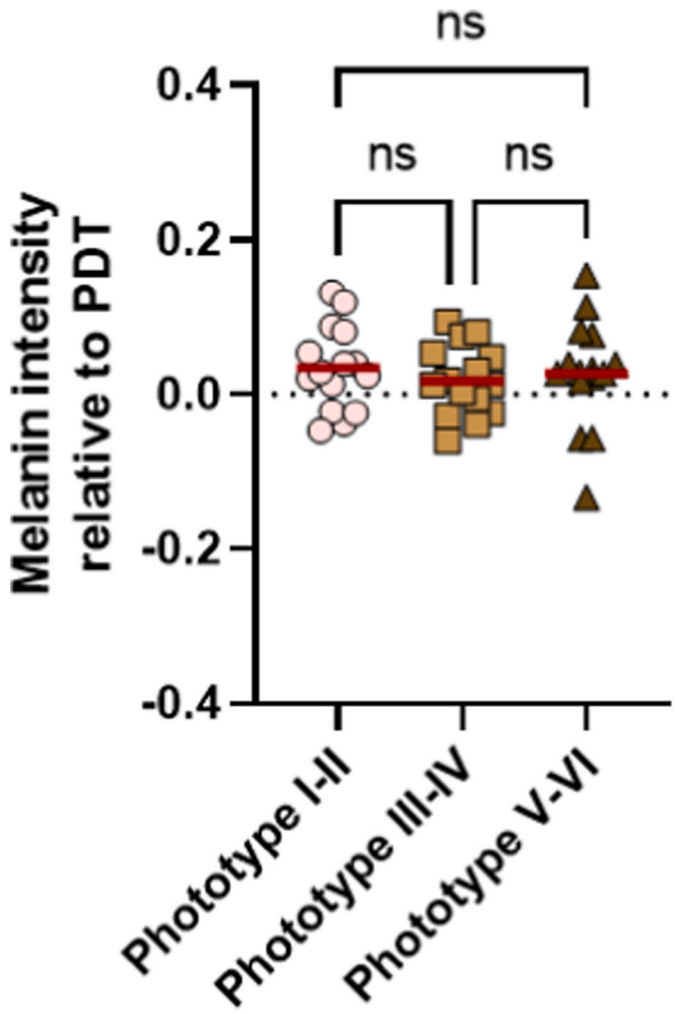

Fig. 5. Influence of the phototype on the melanin signal. 45 healthy volunteers exhibiting a phototype I and II (n = 15), phototype III and IV (n = 15) and phototype V and VI (n = 15) were recruited. Measurements were performed on one arm of those individuals, in a region showing no skin lesion. Each point represents the measurement performed on each individual volunteer. Red bar represents the median value. No significant difference in EPR signal intensity was observed between the different groups of skin phototype ($p = 0.75$, One-way Anova). (For interpretation of the references to colour in this figure legend, the reader is referred to the Web version of this article.)

lesions, 66 were benign atypical nevi (including 3 blue nevi), 30 were classified as melanomas, 1 was a basal cell carcinoma (BCC), and 3 were dermatofibromas (DF). The analyzed melanomas were obtained from patients with the following characteristics: (mean [SD] age, 65.3 [12.9] years; 10 women [33.3%]/20 men [66.7%]). Melanomas included nine superficial spreading melanomas (SSM), one nodular melanoma (NM), sixteen lentigo maligna (seven lentigo maligna in situ (LM) and nine invasive lentigo maligna (LMM)), two skin melanoma metastases (MM), and two undifferentiated melanomas (UM). All melanomas were pigmented, and none of the non-pigmented lesions analyzed in this study were diagnosed as melanomas. The EPR spectra displayed an analyzable signal in 92% of the lesions. The reasons for failure to analyze the signal were the absence of the reference peaks of PDT due to motion (n = 4), abnormal EPR signal of the reference peaks due to EPR line shape distortion (n = 2, see spectra in the Supplementary material for patients #27 and 59), abnormal unstable spectra due to motion (n = 1), and a long distance between the coil and lesion due to protective dressing in one case of an advanced ulcerated bloody lesion (n = 1). Overall, we obtained dual data (EPR/histopathology) for 92 lesions, including 62 benign atypical nevi, 26 melanomas, one basal cell carcinoma, and three dermatofibromas. We observed a highly significant difference ($p < 0.0001$, Mann-Whitney test) in melanin content (expressed as the melanin/PDT ratio) when comparing benign atypical nevi (n = 62) and malignant melanomas (n = 26) (Fig. 6A). No clear trend was observed in melanin content when comparing different types of skin lesions (Fig. 6B). A trend to an increase in melanin content was observed when comparing melanoma with high Breslow (higher than 0.8 mm, n = 10) compared to low Breslow (lower than 0.8 mm, n = 16): the melanin content (expressed as melanin/PDT ratio) was 0.128 ± 0.027 and 0.107 ± 0.025 (mean ± standard error) for high Breslow and low Breslow melanomas, respectively, but the difference was not statistically significant ($p = 0.3561$, Mann-Whitney test) (Fig. 6C). Finally, the analysis of pooled data from the study on phototype in healthy volunteers and the study on suspicious lesions showed that the melanin content (expressed as melanin/PDT ratio) was significantly higher than that in all other groups (ANOVA and multiple comparisons Kruskal-Wallis test, Fig. 6D).

4. Discussion

The main achievement of the present study is that we succeeded in noninvasively detecting endogenous free radicals in human beings by EPR for the first time. To date, clinical studies with low-frequency EPR have only been possible after patient administration of an exogenous paramagnetic sensor reporting on its oxygen environment [5,6] or in teeth after an external high irradiation dose [7,8]. While paramagnetic compounds are present in many biological compounds and can be characterized by high-frequency EPR spectrometers (9 GHz or higher),

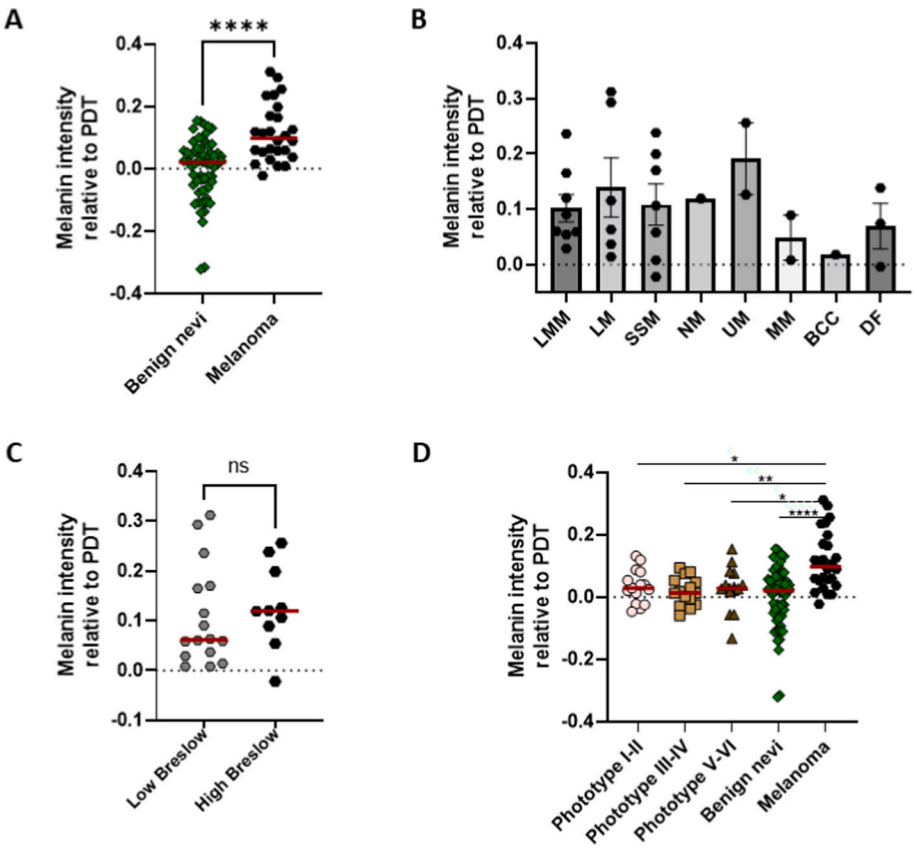

Fig. 6. Results of the EPR study on suspicious lesions. Each point represents the measurement from each single lesion. A: A highly significant difference ($p < 0.0001$, Mann Whitney test) is observed in melanin content when comparing benign atypical nevi ($n = 62$) and melanomas ($n = 26$). Red bars are the medians of the results. B: No clear trend was observed in melanin content when comparing different types of skin lesions. Invasive Lentigo Maligna (LMM), Lentigo Maligna in situ (LM), Superficial Spreading Melanomas (SSM), Nodular Melanoma (NM), undifferentiated melanomas (UM), skin melanoma metastasis (MM), basal cell carcinoma (BCC), dermatofibromas (DF). C: A trend to an increase in melanin content was observed when comparing melanoma with high Breslow (higher than 0.8 mm, $n = 10$) compared to low Breslow (lower than 0.8 mm, $n = 16$), but the difference was not statistically significant ($p = 0.3561$, Mann Whitney test). D: Comparison of pooled data coming from the study on phototype in healthy volunteers and the study on suspicious lesions (benign nevi vs melanomas). Melanin content (expressed as melanin/PDT ratio) was significantly higher in the melanoma group compared to all other groups (Anova and multiple comparisons Kruskal-Wallis test). (For interpretation of the references to colour in this figure legend, the reader is referred to the Web version of this article.)

their detection has so far been impossible using low-frequency spectrometers with limited sensitivity. The selection of melanin as an endogenous free radical was based on the following considerations. First, in contrast to other reactive free radicals, melanin is a highly stable free radical. Second, melanin is present in high concentrations in pigmented skin lesions, compatible with detection using a 1 GHz EPR spectrometer (1 cm depth wave penetration). Third and most importantly, EPR detection of melanin could be highly relevant in the context of clinical applications as a potential differential diagnostic aid for pigmented skin lesions [28]. Our earlier work demonstrated the feasibility of detecting *in vivo* melanin in pigmented melanoma models implanted in anesthetized mice *in vivo* [26,27]. The transfer of this approach to humans is particularly challenging because of the need for an acceptable protocol for patients. In contrast to animal models, in which the optimal configuration for detection can be adapted and optimized over a long period of time, clinical measurements should be performed rapidly and efficiently in humans. In addition, as suspicious lesions can be located in areas prone to motion, it was necessary to use rapid acquisitions compatible with requests for immobility and breath holding. EPR spectra were acquired using a series of two scans of 5 s with relaxing periods between the EPR acquisitions. After the installation of the patient in the magnet, the entire protocol duration was limited to 20 min. Consequently, a limited series of spectra were accumulated, and it was anticipated that the resulting EPR spectra would present a very low signal-to-noise ratio. This prompted us to develop a method that allows the assignment of magnetic field positioning and comparison with a reference signal for quantitative purposes. These two lines of PDT were suitable for this purpose. In addition to its use as a reference during data post-processing, the PDT signal is an excellent marker for assessing the quality of the spectra acquired from patients.

The first trial in healthy volunteers was designed to evaluate the potential impact of skin pigmentation on EPR recordings, which could potentially affect the signal in skin lesions. Using the same conditions as those used for analyzing skin lesions, the signals recorded were not significantly different from the noise, and no significant difference was observed between the different groups despite the obvious differences in melanin content in the epidermis. This result highlights the limited sensitivity of the proposed setup for detecting low melanin concentrations. In turn, this bothering result at first sight could be considered as an advantage to study melanocytic skin lesions, as there was no need for correction due to skin pigmentation. A clinical trial of suspicious melanocytic skin lesions revealed a highly significant difference in melanin content between skin melanomas and benign nevi. This result obtained in a totally noninvasive manner is consistent with earlier results obtained *in vitro* on paraffin-embedded biopsies using high-frequency EPR [28]. Cesareo suggested that spectral variations may be related to qualitative melanin differences occurring in melanoma cells and concluded that this EPR signal may represent a reliable marker for melanoma diagnosis in human histological sections [28]. As the same authors observed differences in melanin content for high and low Breslow melanomas [28], we investigated this possibility using our clinical setup. Although the signal was slightly higher in invasive melanomas with high Breslow (>0.8 mm) than in those with low Breslow (<0.8 mm), the difference was not significant.

Overall, our study should be considered as a proof-of-concept, demonstrating that clinical EPR can noninvasively detect endogenous free radical melanin in melanocytic skin lesions. Using the present configuration, a highly significant difference was observed between malignant melanomas and benign nevi, opening new avenues for evaluating clinical EPR as a potential aid for the diagnosis of pigmented skin lesions. Overall, our study should be considered as a proof-of-concept, demonstrating that clinical EPR can noninvasively detect endogenous free radical melanin in melanocytic skin lesions. Using the present configuration, a highly significant difference was observed between malignant melanomas and benign nevi, opening new avenues for evaluating clinical EPR as a potential aid for the diagnosis of pigmented skin

lesions. In clinical practice, the most useful metrics for measuring accuracy in melanoma detection is the number needed to excise (NNE), calculated as the number of melanocytic lesions excised for every confirmed melanoma. 10 years ago, a large multicenter study revealed that the NNEs were 8.7 and 29.4 for specialized clinical settings (SCS) versus non-specialized clinical settings (NSCS), respectively [33]. The use of digital dermoscopy and reflectance confocal microscopy (RCM) has significantly reduced unnecessary excisions without missing melanoma cases leading now to a NNE between 2.4 and 4 in SCS [34–38]. Of note, due to the limited depth penetration, both methods have limited value to provide information on the Breslow depth. High-frequency ultrasound (HFUS) with transducer frequencies of 20 MHz can produce high resolution images of structures close to the skin surface and inform on the Breslow depth [39]. However, HUFS lacks of specificity regarding the nature of the lesion. Recent developments using multiphoton imaging systems have also shown the potential ability to evaluate the 3D distribution of epidermal melanin content *in vivo* [40]. In this context, the selectivity of EPR for melanin detection as well as its noninvasive nature seem particularly attractive for skin melanoma characterization. We believe that this seminal contribution will inspire scientists in the field. Regarding technological developments, there is clear room for boosting the sensitivity of the method through improvement in instrumentation, for example by developing S-Band (2–3 GHz) bridges compatible with clinical EPR spectrometers, allowing a penetration depth of 2 mm in the skin [41] and/or use of new acquisition modes (i.e., using multiharmonics or rapid-scan), allowing the use of higher modulation amplitude and power [42,43]. Flexible resonators adapted for skin measurements could also be advantageous for minimizing motion artifacts [44]. Finally, as the ultimate goal is to measure the Breslow depth, it will be important to adapt to clinical EPR system resonators and gradients, allowing high-resolution imaging [45] to map the skin penetration of melanin. The observation of a higher signal intensity of melanin in melanoma compared to benign lesions may also stimulate fundamental research to address unsolved issues. An open question is to know why these EPR signals are different. At this point, we can only speculate on possible factors at the origin of changes in EPR signal intensity such as differences in melanin content, in melanin polymer organization, in melanogenesis or in melanin degradation [12,13,46,47]. Because it has been established that the EPR signal could be modulated by the presence of divalent cations, further research is warranted to measure possible variations in metal ions content and metal ions bound to melanin in human melanoma tissues and benign lesions to assess their potential role in EPR signal recorded in physiological conditions [48].

Funding

The acquisition of the clinical EPR spectrometer was funded by the Belgian National Fund for Scientific Research (FNRS). The studies were supported by the Foundation against Cancer (2020–105), and the Fonds spéciaux de recherches (FSR, UCLouvain). Lionel Mignion is postdoctoral researcher of the FNRS, Evelyne Harkemanne has a FNRS fellowship as Medical Doctor Applicant for a PhD, Mohammad Wehbi has a PhD fellowship from the Fonds Spéciaux de Recherches (UCLouvain).

These studies used the facilities of the Nuclear and Electron Spin Technologies (NEST) platform of UCLouvain. The authors thank Karoline Amman, clinical research coordinator of this study. We are grateful for the dedication of all volunteers and patients who participated in these clinical studies.

Author contributions

Conceptualization, B.G.; methodology, L.M., C.M.D., E.H., I.T., N.J., M.W., J.F.B., and B.G.; software, L.M.,C.M.D. and N.J; validation, L.M., I.T., J.F.B., and B.G.; formal analysis, L.M., M.W., and B.G.; investigation, L.M., C.M.D., I.T., E.H., N.J., M.W., J.F.B., and B.G.; resources, I.T., J.F.B., and B.G.; writing—original draft preparation, B.G.; writing—review and editing, L.M., C.M.D., I.T., E.H., N.J., M.W., J.F.B., and B.G.; supervision, I.T., J.F.B., and B.G.; project administration, I.T., J.F.B., and B.G.; funding acquisition, I.T., J.F.B. and B.G.

Declaration of competing interest

The authors declare no conflict of interest.

Data availability

The data generated in this study are available within the article and its supplementary data files.

Appendix A. Supplementary data

Supplementary data to this article can be found online at https://doi.org/10.1016/j.freeradbiomed.2022.08.020.

References

[1] W. Schreiber, S.V. Petryakov, M.M. Kmiec, A.B. Flood, H.M. Swartz, P.E. Schaner, B.B. Williams, In vivo CW-EPR spectrometer systems for dosimetry and oximetry in preclinical and clinical applications, Appl. Magn. Reson. 53 (2022) 123–143.
[2] H. Hirata, H.M. Swartz, RF/Microwave resonators for preclinical and clinical EPR applications: current status and challenges, Appl. Magn. Reson. 53 (2022) 167–191.
[3] H.M. Swartz, Using stable free radicals to obtain unique and clinically useful data in vivo in human subjects, Radiat. Protect. Dosim. 172 (2016) 3–15.
[4] A.B. Flood, V.A. Wood, W. Schreiber, B.B. Williams, B. Gallez, H.M. Swartz, Guidance to transfer 'bench-ready' medical technology into usual clinical practice: case study - sensors and spectrometer used in EPR oximetry, Adv. Exp. Med. Biol. 1072 (2018) 233–239.
[5] J.J. Jeong, T. Liu, X. Yang, M. Torres, J. Lin, W. Schreiber, A.B. Flood, P. Kuppusamy, H.M. Swartz, B.B. Williams, P.E. Schaner, A. Ali, Clinical measurements of oxygen via electron paramagnetic resonance (EPR) during and after breast radiation therapy: preliminary results of baseline evaluations and response to hyperoxygenation, J. Radiol. Radiation Therapy 7 (2019) 1082.
[6] P.E. Schaner, B.B. Williams, E.Y. Chen, J.R. Pettus, W.A. Schreiber, M.M. Kmiec, L. A. Jarvis, D.A. Pastel, R.A. Zuurbier, R.M. DiFlorio-Alexander, J.A. Paydarfar, B. J. Gosselin, R.J. Barth, K.M. Rosenkranz, S.V. Petryakov, H. Hou, D. Tse, A. Pletnev, A.B. Flood, V.A. Wood, K.A. Hebert, R.E. Mosher, E. Demidenko, H. M. Swartz, P. Kuppusamy, First-in-human study in cancer patients establishing the feasibility of oxygen measurements in tumors using electron paramagnetic resonance with the OxyChip, Front. Oncol. 11 (2021), 743256.
[7] B.B. Williams, R. Dong, A.B. Flood, O. Grinberg, M. Kmiec, P.N. Lesniewski, T. P. Matthews, R.J. Nicolalde, T. Raynolds, I.K. Salikhov, H.M. Swartz, A deployable in vivo EPR tooth dosimeter for triage after a radiation event involving large populations, Radiat. Meas. 46 (2011) 772–777.
[8] M. Miyake, Y. Nakai, I. Yamaguchi, H. Hirata, N. Kunugita, B.B. Williams, H. M. Swartz, In-vivo radiation dosimetry using portable L Band EPR: on-site measurement of volunteers in Fukushima prefecture, Japan, Radiat. Protect. Dosim. 172 (2016) 248–253.
[9] B. Gallez, Oxygenation status in normal tissues, pathological tissues and malignant tumors: a pO2 database based on electron paramagnetic resonance (EPR) oximetry measurements, Appl. Magn. Reson. 52 (2021) 1395–1450.
[10] P. Fattibene, F. Callens, EPR dosimetry with tooth enamel: a review, Appl. Radiat. Isot. 68 (2010) 2033–2116.
[11] P.A. Riley, Melanin. *Int. J. Biochem. Cell. Biol.* 29 (1997) 1235–1239.
[12] S. Ito, K. Wakamatsu, Chemistry of mixed melanogenesis–pivotal roles of dopaquinone, Photochem. Photobiol. 84 (2008) 582–592.
[13] T. Sarna, P.M. Plonka, in: S.R. Eaton, G.R. Eaton, L.J. Berliner (Eds.), Biophysical Studies of Melanin" in Biomedical EPR, Part A: Free Radicals, Metals, Medicine, and Physiology. Biological Magnetic Resonance, vol. 23, Springer, 2005, pp. 125–146.
[14] R.C. Sealy, J.S. Hyde, C.C. Felix, I.A. Menon, G. Prota, Eumelanins and pheomelanins: characterization by electron spin resonance spectroscopy, Science 217 (1982) 545–547.
[15] H. Hara, M.H. Lee, H. Chen, D. Luo, K. Jimbow, Role of gene expression and protein synthesis of tyrosinase, TRP-1, lamp-1, and CD63 in UVB-induced melanogenesis in human melanomas, J. Invest. Dermatol. 102 (1994) 495–500.
[16] G.G. Prota, H. Rorsman, A.-M. Rosengren, E. Rosengren, Phaeomelanic pigments from a human melanoma, Experientia 32 (1976) 970–971.
[17] T. Morishima, E. Fukada, Quantitative analysis of eumelanin and pheomelanin in human malignant-melanoma tissues, Arch. Dermatol. Res. 277 (1985) 248–250.
[18] Q. Godechal, G.E. Ghanem, M.G. Cook, B. Gallez, Electron paramagnetic resonance spectrometry and imaging in melanomas: comparison between pigmented and nonpigmented human malignant melanomas, Mol. Imag. 12 (2013) 218–223.
[19] G. Elek, K. Lapis, A. Rockenbauer, ESR investigation of paraffin-embedded ocular melanomas, Br. J. Cancer 41 (1980) 199–203.

[20] H. Katsuda, T. Kobayashi, H. Saito, T. Matsunaga, M. Ikeya, Electron spin resonance imaging of mouse B16 melanoma, Chem. Pharm. Bull. 38 (1990) 2838–2840.
[21] P.M. Plonka, A.T. Slominski, S. Pajak, K. Urbanska, Transplantable melanomas in gerbils (Meriones unguiculatus). II: melanogenesis, Exp. Dermatol. 12 (2003) 356–364.
[22] Q. Godechal, F. Defresne, P. Danhier, P. Leveque, P.E. Porporato, P. Sonveaux, J. F. Baurain, O. Feron, B. Gallez, Assessment of melanoma extent and melanoma metastases invasion using electron paramagnetic resonance and bioluminescence imaging, Contrast Media Mol. Imaging 6 (2011) 282–288.
[23] Q. Godechal, P. Leveque, L. Marot, J.F. Baurain, B. Gallez, Optimization of electron paramagnetic resonance imaging for visualization of human skin melanoma in various stages of invasion, Exp. Dermatol. 21 (2012) 341–346.
[24] P. Danhier, G. De Preter, J. Magat, Q. Godechal, P.E. Porporato, B.F. Jordan, O. Feron, P. Sonveaux, B. Gallez, Multimodal cell tracking of a spontaneous metastasis model: comparison between MRI, electron paramagnetic resonance and bioluminescence, Contrast Media Mol. Imaging 9 (2014) 143–153.
[25] Q. Godechal, L. Mignion, O. Karroum, J. Magat, P. Danhier, R. Morandini, G. E. Ghanem, P. Leveque, B. Gallez, Influence of paramagnetic melanin on the MRI contrast in melanoma: a combined high-field (11.7 T) MRI and EPR study, Contrast Media Mol. Imaging 9 (2014) 154–160.
[26] E. Vanea, N. Charlier, J. Dewever, M. Dinguizli, O. Feron, J.F. Baurain, B. Gallez, Molecular electron paramagnetic resonance imaging of melanin in melanomas: a proof-of-concept, NMR Biomed. 21 (2008) 296–300.
[27] C.M. Desmet, P. Danhier, S. Acciardo, P. Leveque, B. Gallez, Towards in vivo melanin radicals detection in melanomas by electron paramagnetic resonance (EPR) spectroscopy: a proof-of-concept study, Free Radic. Res. 53 (2019) 405–410.
[28] E. Cesareo, L. Korkina, G. D'Errico, G. Vitiello, M.S. Aguzzi, F. Passarelli, J. Z. Pedersen, A. Facchiano, An endogenous electron spin resonance (ESR) signal discriminates nevi from melanomas in human specimens: a step forward in its diagnostic application, PLoS One 7 (2012), e48849.
[29] R.F. Uren, O.E. Nieweg, J.F. Thompson, in: C.M. Balch, M.B. Atkins, C. Garbe, J. E. Gershenwald, A.C. Halpern, J.M. Kirkwood, G.A. McArthur, J.F. Thompson, A. J. Sober (Eds.), "Lymphoscintigraphy in Patients with Melanoma" in Cutaneous Melanoma, sixth ed., Springer, 2020, pp. 205–239.
[30] M.B. Faries, A.J. Cochran, M. McLemore, V.K. Sondak, S.L. Wong, J.F. Thompson, in: C.M. Balch, M.B. Atkins, C. Garbe, J.E. Gershenwald, A.C. Halpern, J. M. Kirkwood, G.A. McArthur, J.F. Thompson, A.J. Sober (Eds.), "Biopsy of the Sentinel Lymph Node" in Cutaneous Melanoma, sixth ed., Springer, 2020, pp. 240–270.
[31] T. Walczak, P. Lesniewski, I. Salikhov, A. Sucheta, K. Szybinski, H.M. Swartz, L-band electron paramagnetic resonance spectrometer for use in vivo and in studies of aqueous biological samples, Rev. Sci. Instrum. 76 (2005), 013107.
[32] T.B. Fitzpatrick, Soleil et peau, J. Med. Esthet. 2 (1975) 33–34.
[33] G. Argenziano, L. Cerroni, I. Zalaudek, S. Staibano, R. Hofmann-Wellenhof, N. Arpaia, R.M. Bakos, B. Balme, J. Bandic, R. Bandelloni, A.M. Brunasso, H. Cabo, D.A. Calcara, B. Carlos-Ortega, A.C. Carvalho, G. Casas, H. Dong, G. Ferrara, R. Filotico, G. Gomez, A. Halpern, G. Ilardi, A. Ishiko, G. Kandiloglu, H. Kawasaki, K. Kobayashi, H. Koga, I. Kovalyshyn, D. Langford, X. Liu, A.A. Marghoob, M. Mascolo, C. Massone, L. Mazzoni, S. Menzies, A. Minagawa, L. Nugnes, F. Ozdemir, G. Pellacani, S. Seidenari, K. Siamas, I. Stanganelli, W.V. Stoecker, M. Tanaka, L. Thomas, P. Tschandl, H. Kittler, Accuracy in melanoma detection: a 10-year multicenter survey, J. Am. Acad. Dermatol. 67 (2012) 54–59.
[34] I. Tromme, L. Sacré, F. Hammouch, C. Legrand, L. Marot, P. Vereecken, I. Theate, P. van Eeckhout, P. Richez, J.F. Baurain, L. Thomas, N. Speybroeck, DEPIMELA study group, Availability of digital dermoscopy in daily practice dramatically reduces the number of excised melanocytic lesions: results from an observational study, Br. J. Dermatol. 167 (2012) 778–786.
[35] J. Dinnes, J.J. Deeks, N. Chuchu, L. Ferrante di Ruffano, R.N. Matin, D.R. Thomson, K.Y. Wong, R.B. Aldridge, R. Abbott, M. Fawzy, S.E. Bayliss, M.J. Grainge, Y. Takwoingi, C. Davenport, K. Godfrey, F.M. Walter, H.C. Williams, Cochrane skin cancer diagnostic test accuracy group. Dermoscopy, with and without visual inspection, for diagnosing melanoma in adults, Cochrane Database Syst. Rev. 12 (2018), CD011902.
[36] N.M. Williams, K.D. Rojas, J.M. Reynolds, D. Kwon, J. Shum-Tien, N. Jaimes, Assessment of diagnostic accuracy of dermoscopic structures and patterns used in melanoma detection: a systematic review and meta-analysis, JAMA Dermatol 157 (2021) 1078–1088.
[37] J. Dinnes, J.J. Deeks, D. Saleh, N. Chuchu, S.E. Bayliss, L. Patel, C. Davenport, Y. Takwoingi, K. Godfrey, R.N. Matin, R. Patalay, H.C. Williams, Cochrane skin cancer diagnostic test accuracy group. Reflectance confocal microscopy for diagnosing cutaneous melanoma in adults, Cochrane Database Syst. Rev. 12 (2018), CD013190.
[38] G. Pellacani, F. Farnetani, S. Ciardo, J. Chester, S. Kaleci, L. Mazzoni, S. Bassoli, A. Casari, R. Pampena, M. Mirra, M. Lai, S. Magi, V.D. Mandel, S. Di Matteo, G. L. Colombo, I. Stanganelli, C. Longo, Effect of reflectance confocal microscopy for suspect lesions on diagnostic accuracy in melanoma: a randomized clinical trial, JAMA Dermatol 158 (2022) 754–761.
[39] A. Kozarova, M. Kozar, I. Tonhajzerova, T. Pappova, E. Minarikova, The value of high-frequency 20 MHz ultrasonography for preoperative measurement of cutaneous melanoma thickness, Acta Dermatovenerol. Croat. 26 (2018) 15–20.
[40] J.R. Vicente, A. Durkin, K. Shrestha, M. Balu, In vivo imaging with a fast large-area multiphoton exoscope (FLAME) captures the melanin distribution heterogeneity in human skin, Sci. Rep. 12 (2022) 8106.
[41] S. Petryakov, M. Chzhan, A. Samouilov, G. He, P. Kuppusamy, J.L. Zweier, A bridged loop-gap S-band surface resonator for topical EPR spectroscopy, J. Magn. Reson. 151 (2001) (2001) 124–128.
[42] M. Gonet, M. Baranowski, T. Czechowski, M. Kucinska, A. Plewinski, P. Szczepanik, S. Jurga, M. Murias, Multiharmonic electron paramagnetic resonance imaging as an innovative approach for in vivo studies, Free Radic. Biol. Med. 152 (2020) 271–279.
[43] G.R. Eaton, S.S. Eaton, Advances in rapid scan EPR spectroscopy, Methods Enzymol. 666 (2022) 1–24.
[44] W. Schreiber, S.V. Petryakov, M.M. Kmiec, M.A. Feldman, P.M. Meaney, V. A. Wood, H.K. Boyle, A.B. Flood, B.B. Williams, H.M. Swartz, Flexible, wireless, inductively coupled surface coil resonator for EPR tooth dosimetry, Radiat. Protect. Dosim. 172 (2016) 87–95.
[45] D.A. Komarov, A. Samouilov, H. Hirata, J.L. Zweier, High fidelity triangular sweep of the magnetic field for millisecond scan EPR imaging, J. Magn. Reson. 329 (2021), 107024.
[46] R.M. Slominski, T. Sarna, P.M. Plonka, C. Raman, A.A. Brozyna, A.T. Slominski, Melanoma, Melanin, and Melanogenesis: The Yin and Yang relationship, Front. Oncol. 12 (2022), 842496.
[47] K. Wakamatsu, J.H. Zippin, S. Ito, Chemical and biochemical control of skin pigmentation with special emphasis on mixed melanogenesis, Pigment Cell Melanoma Res 34 (2021) 730–747.
[48] T. Sarna, H.M. Swartz, A. Zadlo, Interaction of melanin with metal ions modulates their cytotoxic potential, Appl. Magn. Reson. 53 (2022) 81–103.